Proceedings of International Conference on Heat Exchanger Fouling and Cleaning - 2011 (Peer-reviewed)
June 05 - 10, 2011, Crete Island, Greece
Editors: M.R. Malayeri, H. Müller-Steinhagen and A.P. Watkinson

Published online
www.heatexchanger-fouling.com

INCREASED SHEAR STRESS IN ANNULAR SWIRLING FLOW FOR REDUCED FOULING RATE

H. Pálsson[1], F. Beaubert[2] and S. Lalot[2]

[1] University of Iceland, Hjarðarhaga 2-6, 107 Reykjavik, Iceland, halldorp@hi.is (Corresponding author)
[2] UVHC, Campus Mont Houy, 59313 Valenciennes Cedex 9, France,

ABSTRACT

Fouling buildup in circular heat exchanger pipes is a common problem in the industry. Various methods have been proposed, amongst others to increase the shear stress of the fluid near the pipe wall. This is known to reduce fouling rate as well as increase the heat transfer rate of heat exchangers. In this paper, the effect of fouling rate reduction is investigated by increasing friction in a circular pipe. This is done by inducing swirling flow at the pipe entrance, which in turn increases velocities close to the wall and consequently the shear stress.

Results are obtained from a three dimensional finite volume CFD code, where the pipe is modeled along with a swirling device at the entrance. Flow conditions are set to the laminar regime, where the effects of swirling flow are much more influential than in turbulent flow. It is concluded that considerable increase in friction can be obtained, but at the cost of increase in pressure drop.

INTRODUCTION

Heat exchangers are widely used in diverse applications with the purpose of transferring heat from one fluid to another in an effective way. Many variations exist in both size and shape, but the most common heat exchangers are of the shell and tube type as well as plate heat exchangers. The main concerns involving heat exchanger design are: cost, effectiveness, weight and size, and finally resistance to fouling and corrosion.

In most cases by far, the fluid flow inside heat exchangers is in the turbulent regime, since heat transfer rate is much higher than in laminar flow. However, in some specific applications laminar flow can be expected, especially if the fluids are highly viscous or if the pipes used for transport are small. The consequences of this are obviously low heat transfer rate in the laminar regime and increased rate of fouling. On one hand the latter is included as the removal term in the famous Ebert and Panchal equation (e.g. Wilson et al., 2005) and on the other hand this is confirmed by the fact that the initial fouling rate is higher for low Reynolds number than for high Reynolds numbers as shown on Figure 5 in (Watkinson and Li, 2009).

Different methods exist for increasing heat transfer in laminar and mildly turbulent flows. A widely used method is to install helical spirals or other kinds of fins, either inside heat exchanger tubes or on the outside; see e.g. (Eiamsa-ard et al. 2006) and (Eiamsa-ard et al., 2010). This perturbs the flow and increases the heat transfer considerably along the pipe. Another effect is reduction in fouling rate, since the increased shear stress at the walls can slow the buildup of deposits in particular types of fouling situations as shown in (Krueger and Pouponnot, 2009). Nevertheless, one drawback of such installation is, apart from the increased pressure drop in the flow, increased complexity of constructing the heat exchangers and cleaning them if necessary; see (Manglik and Bergles, 2003). Also, in some areas close to the insertion spirals, low velocity can be experienced and thus local fouling might be a problem.

One particular method for increasing shear stress along pipe walls is to induce rotating or swirling flow. Swirling flow in tubes has been widely studied, both for the turbulent regime (Escue and Cui, 2010) as well as the laminar regime; see e.g. (Marner and Bergles, 1989), (Saha et al., 2001) and (Wongcharee and Eiamsa-ard, 2011). In this case, a rotating momentum is added to the flow in a circular pipe, turning the fluid either clockwise or counterclockwise in addition to the axial velocity along the pipe. This results in added shear stress at the walls and also in increased mixing in the fluid core section, thus increasing the heat transfer from the fluid to the walls. Also, if the flow is set to circular motion at a given cross section, the circular movement continues along a considerable distance downstream in the pipe. The advantage of inducing the swirling flow at one cross section is that a large portion of the downstream pipe wall is free of any insertion objects that might contribute to problems regarding fouling and cleaning of the pipes. But finally it should be noted that the swirling flow induction is not free of charge, some pressure drop is always present in the induction section and fouling can also occur there, based on the induction device used.

The purpose of this work is to investigate the effects of including a specific swirling inducing device into a heat exchanger pipe within a laminar flow regime; using water for the fluid. Effects on shear stress, and downstream

duration of the swirling effects are investigated quantitative using a three dimensional computational fluid dynamics (CFD) model. A special consideration is given on the increased shear stress. The cost of the increased pressure loss will not be studied in detail, as it should be compared to the cost of dismantling and cleaning.

METHODS AND THEORY

In this section, the theoretical background for the flow calculations is presented. This covers both the mathematical definitions as well as the numerical model and individual methods used.

Mathematical representation of the flow

Consider incompressible laminar steady flow of viscous fluid with constant transport properties. The governing equations consist of the momentum part

$$\vec{\mathbf{u}} \cdot \nabla \vec{\mathbf{u}} + \frac{1}{\rho} \nabla p = \nu \, \nabla \cdot \nabla \vec{\mathbf{u}} \tag{1}$$

accompanied by the continuity equation

$$\nabla \cdot \vec{\mathbf{u}} = 0 \tag{2}$$

The flow variables are velocity $\vec{\mathbf{u}}$ in m/s and pressure p in N/m^2. In the case of incompressible flow, the kinematic pressure p' can be used to eliminate the density ρ, since $p = \rho \, p'$. By using the kinematic pressure, the only transport property to be specified is the kinematic viscosity ν in m/s^2.

Here it is assumed that the fluid is Newtonian and thus there is a simple relation between the symmetric strain tensor $\nabla \vec{\mathbf{u}}$ and the tangential shear stress vector $\vec{\boldsymbol{\tau}}$. The kinematic wall shear stress $\vec{\boldsymbol{\tau}}'$ is related to the velocity by

$$\vec{\boldsymbol{\tau}}' = \nu \left(\vec{\mathbf{n}} \cdot \nabla \vec{\mathbf{u}} \right) \tag{3}$$

where $\vec{\boldsymbol{\tau}} = \rho \, \vec{\boldsymbol{\tau}}'$ and $\vec{\mathbf{n}}$ is the outward unit normal vector of the wall. Note that in comparing the shear stress, the modulus of $\vec{\boldsymbol{\tau}}'$ should be considered in general.

Boundary conditions for $\vec{\mathbf{u}}$ and p must be specified in an appropriate manner for the current problem. At the pipe walls (as well as walls of the swirling device), the no-slip condition $\vec{\mathbf{u}} = \vec{\mathbf{0}}$ is used, as well as specifying $\vec{\mathbf{n}} \cdot \nabla p = 0$ to fulfill continuity.

At the inlet, the conditions are specified as expected balanced flow profile for a steady non-swirling flow. For normal pipes, the flow will follow a parabolic profile normal to the inlet surface (Eq. 4):

$$\vec{\mathbf{u}} = 2\bar{u} \left(1 - \frac{r^2}{r_0^2} \right) \vec{\mathbf{z}} \tag{4}$$

where r is the distance from the center line of the pipe of radius r_0 and $\bar{u}$ is the mean inlet velocity. Other cases need special treatment, as shown in the following subsection.

At the outlet the flow can still be in a swirling motion even though the outlet is positioned far away from the swirling device. This would normally results in a low pressure zone near the pipe center because of centrifugal effects, so that the normal procedure of specifying the outlet pressure $p = 0$ results in small errors at the exit. However, this should not affect the solution much, near the device itself and in the regions where its effects are significant.

Laminar flow in an annulus

In the particular case investigated in this paper, the flow takes place in an annulus, where a pipe of a relatively small diameter is located in the center of the main pipe. The reason for such a setup is that multiple swirling devices would in reality be inserted into long heat exchanger pipes, requiring them to be connected in a series with an appropriate axial distance. One drawback is that this will increase the pressure drop in the pipe to some extent.

An analytical solution for the velocity profile and the wall shear stress can be derived from the steady momentum equations in cylindrical coordinates. Assuming axial flow only (inlet conditions into the annulus) the angular and radial velocities are zero and changes along the axis are also zero. Consequently the angular and radial momentum equations simplify to $\partial p / \partial \theta = 0$ and $\partial p / \partial r = 0$ and the axial momentum becomes

$$\frac{\partial p}{\partial z} = \mu \frac{1}{r} \frac{\partial}{\partial r} \left(r \frac{\partial u_z}{\partial r} \right) \tag{5}$$

Now since $\frac{\partial p}{\partial r} = 0$ the first term in Eq. 5 must be constant, and therefore the equation simplifies to a second order ordinary differential equation (ODE) with a constant source term $S = -\frac{1}{\mu} \frac{\partial p}{\partial z}$. The solution of the ODE is

$$u_z(r) = \frac{S}{4} \left(r_0^2 - r^2 - \frac{\left(r_0^2 - r_i^2 \right) \ln\left(\frac{r}{r_0} \right)}{\ln\left(\frac{r_i}{r_0} \right)} \right) \tag{6}$$

A possible condition for the flow is to set the volumetric flow equal to a standard case, as shown in Eq. 4, and thus including $\bar{u}$ as a parameter in the equations. This conditions requires that

$$\bar{u} \pi \, r_0^2 = 2\pi \int_{r_i}^{r_o} u_z(r) \, r dr \tag{7}$$

and by evaluating the integral and inserting Eq. 6 into Eq. 7 the result is

$$\bar{u}\pi\, r_0^2 = \frac{\pi\, S}{8} r_0^4 \left(1 - \frac{r_i^4}{r_o^4} + \frac{\left(1 - \frac{r_i^2}{r_o^2}\right)^2}{\ln\left(\frac{r_i}{r_o}\right)} \right) \tag{8}$$

Finally, by defining $\eta = \frac{r_i}{r_o}$, the velocity becomes

$$u_z(r) = 2\bar{u} \left(\frac{1 - \left(\frac{r}{r_0}\right)^2 - \frac{\left(1-\eta^2\right)\ln\left(\frac{r}{r_0}\right)}{\ln(\eta)}}{1 - \eta^4 + \frac{\left(1-\eta^2\right)^2}{\ln(\eta)}} \right) \tag{9}$$

Now the wall shear stress can be acquired at the outer pipe wall which is of main interest by evaluating $\tau_w = -\mu \frac{du_z}{dr}$ which results in

$$\tau_w = \frac{2\bar{u}\mu}{r_o} \left(\frac{2 + \frac{\left(1-\eta^2\right)}{\ln(\eta)}}{1 - \eta^4 + \frac{\left(1-\eta^2\right)^2}{\ln(\eta)}} \right) \tag{10}$$

at the outer wall which is of main interest. However, it should be noted that the shear stress at the inner wall is much higher than the stress on the main outer wall. Finally, the pressure drop along the annulus can be computed as

$$\frac{\partial p}{\partial z} = -\frac{8\bar{u}\mu}{r_o^2\left(1-\eta^2\right)\left(1 + \eta^2 + \frac{\left(1-\eta^2\right)}{\ln(\eta)}\right)} \tag{11}$$

Equations 10 and 11 can be compared both to a case where there is no pipe in the center of the main pipe, as well as to numerical computations for swirling flows.

It can be easily checked that Equations 9 to 11 reduce to the well known laminar pipe equations when there is no inner surface, i.e. when $\eta = 0$.

Numerical procedures

A steady laminar solution of the Navier-Stokes equations was obtained by using the open source CFD software OpenFOAM, version 1.7.x, developed by OpenCFD Ltd (see http://www.openfoam.com). The software incorporates a solver for this particular problem, based on velocity-pressure coupling, or the SIMPLE algorithm (Semi-Implicit Method for Pressure-Linked Equations), see e.g. (Patankar, 1980). The overall numerical approach in OpenFOAM is the finite volume method.

Various discretization schemes are available for the spatial derivatives in Eqs. (1-2). The most simple scheme for the advection part in Eq. 1 is first order upwind, which is usually very stable in spite of inaccuracy when used in advection dominated problems. Here, a relatively fine mesh has been selected and flow velocities are generally small, which justifies the use of first order upwind as an advective discretization scheme $(\vec{\mathbf{u}} \cdot \nabla \vec{\mathbf{u}})$.

The diffusive part of Eq. 1 as well as the diffusive pressure equation in the SIMPLE algorithm are solved by using a Gauss integration approach for the Laplacian, with a correction due to non-orthogonality of the mesh. Other necessary interpolation procedures are linear, such as determination of various fluxes needed in the calculations.

Boundary conditions are applied in a consistent manner in the numerical procedures, whether they are given values of $\vec{\mathbf{u}}$ and p or normal derivatives. In particular, the numerical algorithms in OpenFOAM utilize corrections at boundaries to ensure that Eq. 2 is fulfilled everywhere in the computational domain and especially at boundaries.

CASE STUDY DESCRIPTION

Numerical simulations in this work were performed on a specific case of an annulus with a swirling device near the inlet point. The dimensions were chosen so they would represent a realistic and typical case for a heat exchanger tube with water flowing in the center. Figure 1 shows the main dimensions used for the case.

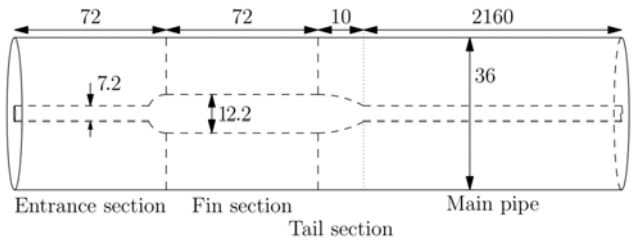

Fig. 1 A heat exchanger pipe with an annular water passage. All dimensions are in millimeters

The swirling device itself is a hydrofoil, consisting of a solid surface in the center which is attached to thin fins that extend from the center to the main pipe wall. The number of blades in the current case has been set to four and they are twisted along the flow axis in order to direct the flow into a swirling motion. Figure 2 illustrates the definition of the twisting geometry, which consists of a Bézier curve with a given inlet and outlet angles. The parameter D denotes the main pipe diameter (which is 36 mm in the test case) and h is the length of the fin section. Other parameters in the figure can be adjusted to acquire the desired inlet and outlet angles of the device, as well as the twisting angle around the axis.

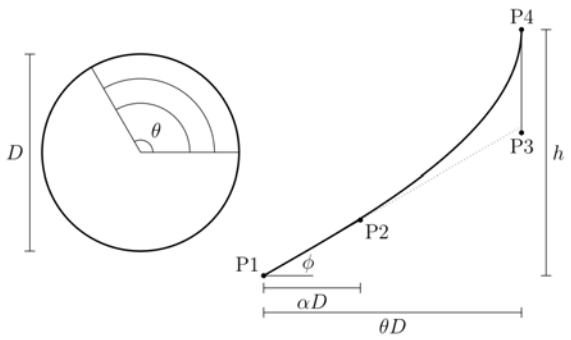

Fig. 2 Twisting curvature of the swirler blades in the axial direction

Finally, Fig. 3 shows how the combined device looks like for the case of four fins, but without the inner pipe wall. The twisting angle θ for this case is 90°. The overall shape of the device is subject to refinement and optimization, in order to minimize the pressure drop while inducing enough swirling motion, but this is a subject for further studies.

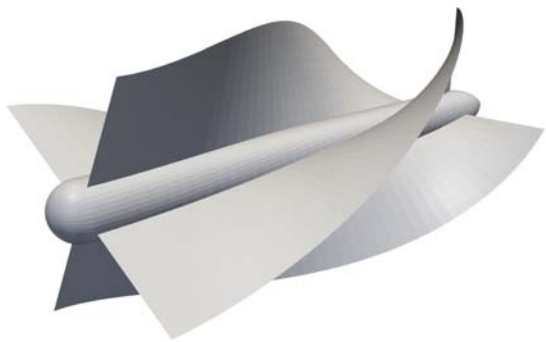

Fig. 3 A three dimensional illustration of the swirling device, including a center and four fins

RESULTS

The main results of the study were focused on the increased shear stress as a result of the swirling flow. The fact that an annular flow passage was used requires the comparison to be performed with the annulus as a base case, thus using Eqs. (9-11) for the comparison. The kinematic viscosity of the fluid was set to $1.004 \cdot 10^{-6}\ \mathrm{m}^2/\mathrm{s}$ and the flow velocity was selected to fulfill $\mathrm{Re} = 2000$, ensuring laminar flow at the inlet of the pipe; see the "discussion" section of the paper for the influence of the swirler on the downstream flow regime.

Mesh construction and dependency

The heat exchanger pipe with a single swirling device was modeled in three dimensions, using the finite volume meshing program GMSH (see http://www.geuz.org/gmsh/).

For the current case, four fins have been selected in the mesh device, and since the flow is steady, only one fourth of the pipe has to be specified as a computational domain. This saves a lot of computation time, and is implemented by using cyclic boundary conditions on the domain faces intersecting the annular flow passage. Figure 4 shows the mesh geometry for a case with a total of 538620 computational cells.

In order to be able to estimate the accuracy of the wall shear stress calculations, the effects of using a mesh of different complexity has been investigated. This was done by comparing the wall shear stress for three different mesh densities, since the stress is the main parameter to be acquired in the study. Table 1 shows the results for three densities, where only the main pipe wall is referred to in the stress calculations. The results for the maximum stress as well as the mean stress (averaged over the surface) are in good agreement, indicating that the coarsest mesh is sufficient. The kinematic pressure difference between inlet and outlet is also shown, indicating good convergence for the pressure as well. The decrease of the value of the minimum stress is due to a phenomenon close to the Kutta-Jukowski condition: at the trailing edge of the blades the velocity is close to zero (hence the shear stress); this is due to the mixing of the two boundary layers.

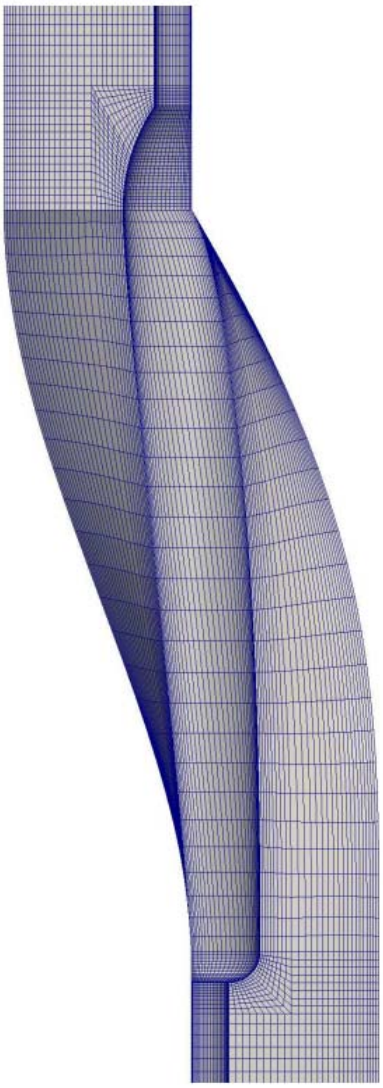

Fig. 4 An example mesh of the pipe, close to the swirling device

Table 1. Effect of different mesh densities on wall shear stress. Note that $\|\vec{\tau}'\|$ and p' are kinematic values in mm^2/s^2

Number of cells	$\|\vec{\tau}'\|_{min}$	$\|\vec{\tau}'\|_{max}$	$\|\vec{\tau}'\|_{avg}$	p'_{inlet}
538620	0.805	118	23.1	9553
1210248	0.37	121	23.7	9622
2231370	0.31	123	24.4	9786

Wall shear stress

The shear stress was calculated on the outer pipe wall, which is the heat exchange area affected by the increase in shear. One important aspect of the increased shear is the magnitude in relation to the position of the fins in the swirling device. Figure 5 shows the distribution of $\frac{\|\vec{\tau}\|}{\tau_0}$ where τ_0 denotes the shear stress without a swirler, at given distances from the swirling section. Close to the fins, their effect can clearly be seen, but further along this effect is reduced because of diffusive effects in the flow (viscosity).

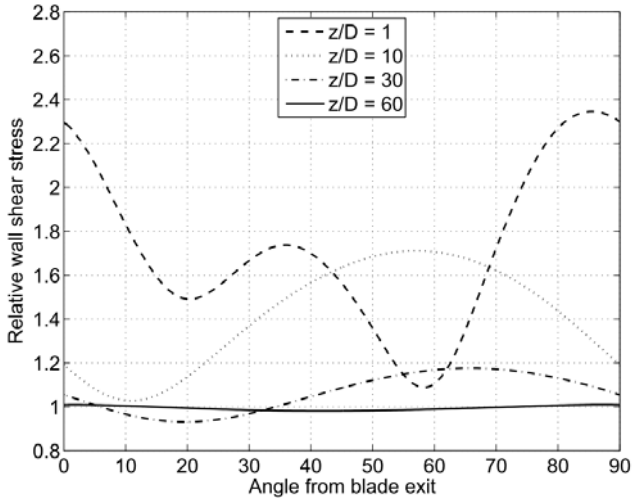

Fig. 5 Relative increase in shear stress for selected cross sections along the pipe axis

Also note that when Eq. 10 is compared to the standard shear stress in a normal pipe (no pipe in the center) which is given as

$$\tau_w = \frac{4\bar{u}\mu}{r_0} \qquad (12)$$

Note also that using $\eta = 0.2$, the shear stress for an annulus without swirling flow is a factor 1.65 higher than for a normal pipe. Thus the computed stress in Fig. 5 must be multiplied by that factor for a comparison with an empty main pipe.

Figure 6 on the other hand shows the mean angular shear stress as a function of the distance from the swirler exit. This is particularly important, since it shows the apparent downstream distance where the swirling effects are actually of significant importance. The figure clearly shows that the effect lasts for quite a distance, up to 45 times the pipe diameter. It can be concluded that up to this position, the removal term of the Ebert and Panchal equation is increased, reducing the fouling factor rising rate.

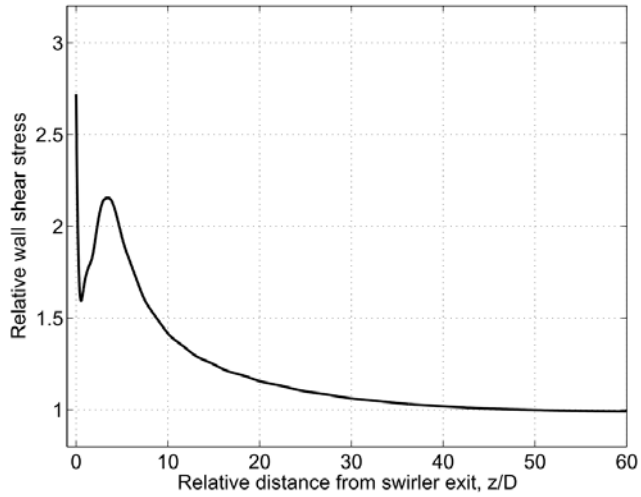

Fig. 6 Relative increase in mean shear stress along the flow axis

In practice, heat exchanger tubes are quite long. They can span up to 500 times their diameter. Thus, it would be necessary to include at least 10 swirlers inside the tubes, as Fig. 6 indicates. But to be able to remove them for cleaning (the swirlers do not avoid deposits, just reduce the rate), they have to be mechanically linked. This explains the inner tube in the simulations as mentioned before.

It must be noted that to keep a very high wall shear stress, the swirlers must be separated by less than the distance where the swirl effect is no longer present. Hence, the inlet angle of the swirlers (but the first one), should be designed so that it fits with the swirling velocity from the next swirler upstream.

Pressure drop

As mentioned before, one of the drawbacks of including a swirling device into the heat exchanger pipes is the additional head loss, or pressure drop what will inevitably be present. Figure 7 shows the difference clearly when compared to Eq. 11 in an annulus. The fluctuations are quite fast close to the fins, but disappear later on.

In fact, as can be seen in Figure 1, the swirler studied here is twice as long as the diameter of the main pipe. And it can be observed on Fig. 7 that for the first oscillations of the curve, the peaks are separated by a relative distance close to 2 (which is the ratio of the swirler length to the pipe diameter).

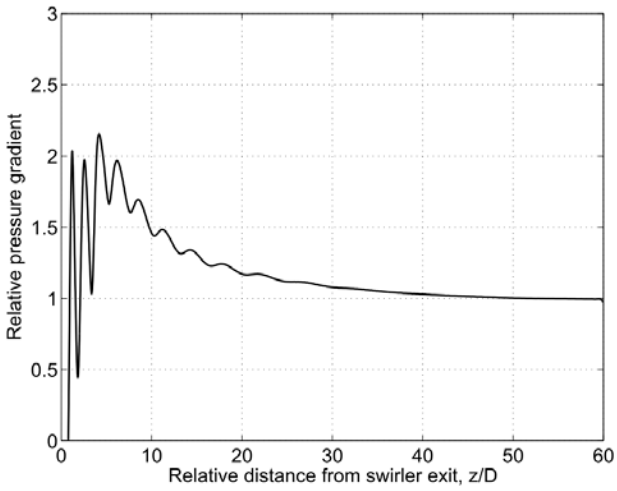

Fig. 7 Relative pressure change $\partial p / \partial z$ along the pipe, compared to an annulus with no swirling device

Figure 8 shows that there is a clear jump in the swirler section, followed by a pressure increase because of velocity changes; pressure drop in a standard circular tube is shown for reference.

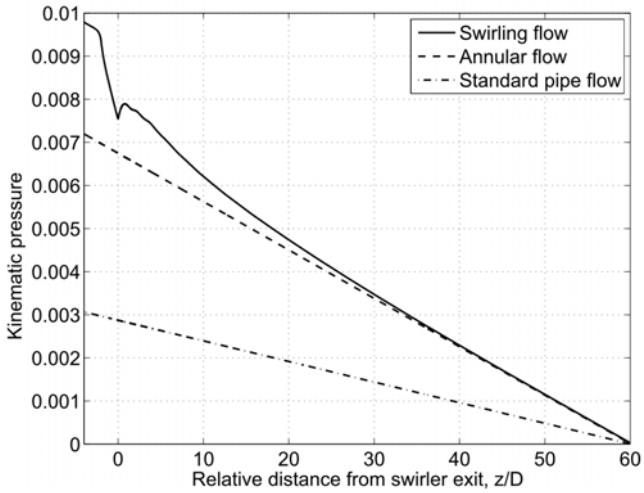

Fig. 8 Comparison of the kinematic pressure between the standard pipe flow and the annular flows (with and without the swirler)

Note that all the pressure calculations are based on a mean pressure on the outer pipe wall, thus not including possible pressure variations in fixed cross sections. But it must be noted that a previous computation taking account of a main pipe length of 120 times the diameter has shown that the swirl effect has disappeared at 60 times the diameter, so that it is legitimate to assume that the length of the computational domain is sufficient for this particular swirler.

DISCUSSION

As stated beforehand, only one fourth of the geometry has been modeled. To be sure that the solver handles this type of boundary condition in swirling flows, a comparison has been made between a full revolution (360°) and what has been chosen afterwards (90°). Figure 9 compares the azimuthal distribution of relative wall shear stress on the outer pipe wall at $z/D = 2.78$. This figure clearly shows the innocuousness of cyclic boundary conditions on the results.

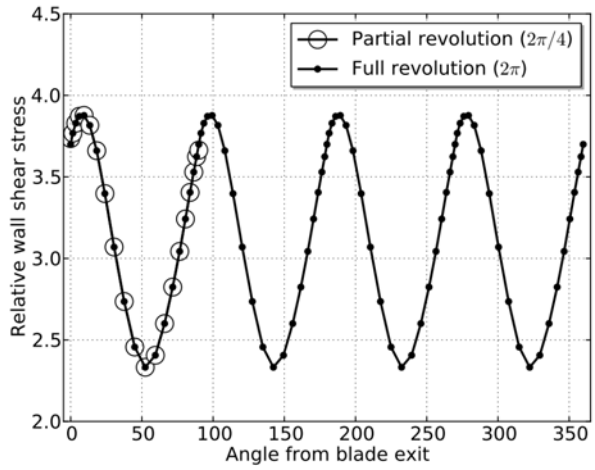

Fig. 9 Comparison between results for cyclic boundary conditions and a full computational domain

Since the flow is close to transition between laminar and turbulent regime (Re=2000) the sensitivity of the flow to turbulence was investigated by using a Launder and Sharma (Launder and Sharma, 1974) $\kappa - \varepsilon$ model without wall functions. This low-Re turbulence model fully resolves the boundary layers but requires a refined mesh with the first cell at the walls at a low wall coordinate: $y^+ < 1$. In the present simulation the maximum y^+ on the pipe walls is less than 0.01 and thus ensures that the viscous sublayer is correctly resolved. Figure 10 shows that the Launder and Sharma low Re turbulence model has no influence on the wall shear stress distribution on the outer pipe wall and thus indicates that the flow remains laminar downstream of the swirler. So, it is legitimate to use the laminar model for all computations.

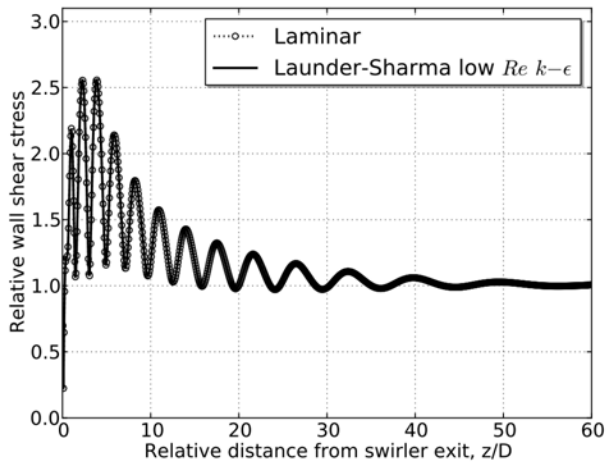

Fig. 10 Comparison between results for laminar conditions and for a low Reynolds turbulence model

Figure 11 shows the distribution of the relative wall shear stress $\|\vec{\tau}\| / \tau_0$ on a line ($y = 0$) of the outer pipe wall to estimate the effect of the Reynolds number on the flow. It is clear that the influence of swirler device is lost when $z / D > 10$ for Re=500 which is due to the larger effect of the viscosity for this Reynolds number.

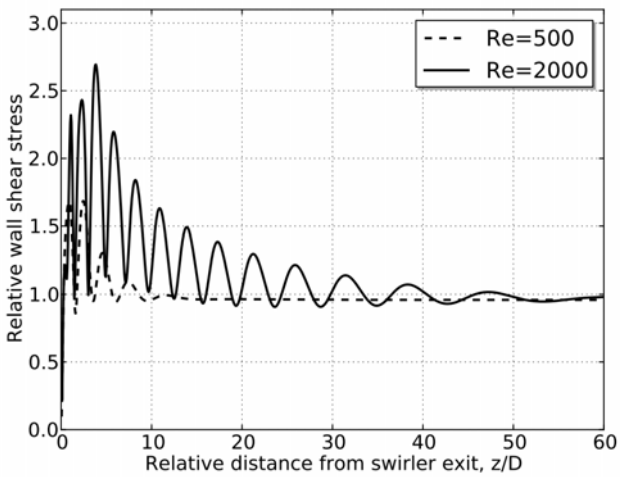

Fig. 11 Illustration of the effect of the Reynolds number on the relative wall shear stress

CONCLUSIONS

In the present work, methods for increasing shear stress in laminar pipe flow have been considered, based on swirling flow. The application is related to heat exchanger tubes, which can be subject to fouling. Previous studies have shown that the increased wall shear stress not only improves heat transfer, but can also reduce fouling rate considerably.

Only one particular shape of a swirl induction device has been presented in the study, but it is clear that dimensions and shape of such a device should be optimized with the purpose of maximizing heat transfer while keeping the increased pressure loss at a minimum.

Results from CFD computations show that the shear stress can be doubled for axial distances up to about 10 diameters. On the whole, the swirling effect lasts for about 10 to 45 pipe diameters depending on the Reynolds number.

The insertion of swirling devices increases pressure drop considerably in the pipes. However, the benefits of increased heat transfer and fouling resistance can outweigh the negative effects of the pressure drop.

Further studies will include heat transfer calculations as well as an optimization of the swirling device shape with respect to both the shear stress and the pressure drop.

ACKNOWLEDGMENTS

This work is carried out in the framework of an international project: FISF (Fundamentals of Internal Swirling Flows). This project is partly sponsored by the University of Valenciennes. This financial support is greatly acknowledged.

NOMENCLATURE

D	pipe diameter, m
h	height of the swirler, m
$\vec{\mathbf{n}}$	unit normal vector, dimensionless
Pi	control point $i \in \{1,2,3,4\}$
p	pressure, N / m^2
p'	kinematic pressure, m^2 / s^2
Re	Reynolds number, dimensionless
r	radius, m
S	source term in equation 6, $m^{-1}s^{-1}$
$\vec{\mathbf{u}}$	velocity vector, m / s
$\bar{u}$	mean velocity, m / s
u_z	velocity in the z direction, m / s
y^+	wall coordinate, dimensionless
z	coordinate along the axis of the tube, m
$\vec{\mathbf{z}}$	unit vector of the tube axis, dimensionless
α	angle, ° or rd
ε	dissipation rate, m^2 / s^3
ϕ	angle, ° or rd
η	radius ratio, dimensionless
κ	turbulent kinetic energy, m^2 / s^2
μ	dynamic viscosity, kg / m.s
ν	kinematic viscosity, m^2 / s
θ	angle, ° or rd
ρ	density, kg / m^3
$\vec{\tau}$	shear stress vector, N / m^2
$\vec{\tau}'$	kinematic shear stress vector, m^2 / s^2
∇	nabla operator
$\cdot$	inner product

Subscript

avg	average
i	inner
inlet	at the inlet
max	maximum
min	minimum
o	outer
w	wall

REFERENCES

Eiamsa-ard, S., Thianpong, C., Eiamsa-ard, P., and Promvonge, P. (2010). Thermal characteristics in a heat exchanger tube fitted with dual twisted tape elements in

tandem. International Communications in Heat and Mass Transfer, 37(1):39–46.

Eiamsa-ard, S., Thianpong, C., and Promvonge, P. (2006). Experimental investigation of heat transfer and flow friction in a circular tube fitted with regularly spaced twisted tape elements. International Communications in Heat and Mass Transfer, 33(10):1225–1233.

Escue, A. and Cui, J. (2010). Comparison of turbulence models in simulating swirling pipe flows. Applied Mathematical Modelling, 34(10):2840–2849.

Krueger, A. and Pouponnot, F. (2009). Heat exchanger performance enhancement through the use of tube inserts in refineries and chemical plants - Succesful applications: Spirelf, Turbotal and Fixotal systems. In Muller-Steinhagen, H., Malayeri, M. R., and Watkinson, A. P., editors, Proceedings of International Conference on Heat Exchanger Fouling and Cleaning VIII, volume 2009, pages 399–406, Schladming, Austria.

Launder, B. E. and Sharma, B. I. (1974), "Application of the Energy-Dissipation Model of Turbulence to the Calculation of Flow Near a Spinning Disc", Letters in Heat and Mass Transfer, Vol. 1, No. 2, pp. 131-138.

Manglik, R. M. and Bergles, A. E. (2003). Swirl flow heat transfer and pressure drop with twisted-tape inserts, volume 36 of Advances in Heat Transfer, chapter Volume 36, pages 183–266. Elsevier.

Marner, W. J. and Bergles, A. E. (1989). Augmentation of highly viscous laminar heat transfer inside tubes with constant wall temperature. Experimental Thermal and Fluid Science, 2(3):252–267.

Patankar, S. V. (1980). Numerical Heat Transfer and Fluid Flow. Hemisphere Pub. Corp.

Saha, S. K., Dutta, A., and Dhal, S. K. (2001). Friction and heat transfer characteristics of laminar swirl flow through a circular tube fitted with regularly spaced twisted-tape elements. International Journal of Heat and Mass Transfer, 44(22):4211–4223.

Watkinson, A. P. and Li, Y.-H. (2009). Fouling characteristics of a heavy vacuum gas oil in the presence of dissolved oxygen. In Muller-Steinhagen, H., Malayeri, M. R., and Watkinson, A. P., editors, Proceedings of the International Conference on Heat Exchanger Fouling and Cleaning VIII, volume 2009, pages 27–32, Schladming, Austria.

Wilson, D. I., Polley, G. T., and Pugh, S. J. (2005). Ten years of Ebert, Panchal and the 'threshold fouling' concept. In Muller-Steinhagen, H., Malayeri, M. R.,and Watkinson, A. P., editors, Heat Exchanger Fouling and Cleaning - Challenges and Opportunities, Kloster Irsee, Germany. ECI Symposium Series.

Wongcharee, K. and Eiamsa-ard, S. (2011). Friction and heat transfer characteristics of laminar swirl flow through the round tubes inserted with alternate clockwise and counter-clockwise twisted-tapes. International Communications in Heat and Mass Transfer, 38(3):348–352.